Finite element computation for scattering problems of micro-hologram using DtN map

Mizuyama, Yosuke
Panasonic Boston Laboratory

Shinde, Takamasa
Fujitsu Advanced Technologies Limited

Tabata, Masahisa
Faculty of Mathematics, Kyushu University

Tagami, Daisuke
Faculty of Mathematics, Kyushu University

https://hdl.handle.net/2324/15573

出版情報：MI Preprint Series. 2009-35, 2009-10-08. 九州大学大学院数理学研究院
バージョン：
権利関係：

MI Preprint Series

Kyushu University
The Global COE Program
Math-for-Industry Education & Research Hub

Finite element computation for scattering problems of micro-hologram using DtN map

Yosuke Mizuyama, Takamasa Shinde, Masahisa Tabata and Daisuke Tagami

MI 2009-35

(Received October 8, 2009)

Faculty of Mathematics
Kyushu University
Fukuoka, JAPAN

Finite element computation for scattering problems of micro-hologram using DtN map

Yosuke Mizuyama[1], Takamasa Shinde[2], Masahisa Tabata[3], and Daisuke Tagami[3]

[1]Panasonic Boston Laboratory; 2 Wells Avenue, Newton, MA 02459, USA

[2]Fujitsu Advanced Technologies Limited; 4-1-1, Kamikodanaka, Nakahara-ku, Kawasaki, 221-8588 JAPAN

[3]Faculty of Mathematics, Kyushu University; 744, Motooka, Nishi-ku, Fukuoka, 819-0395 JAPAN

E-mail: `mizuyamay@us.panasonic.com`, `{tabata,tagami}@math.kyushu-u.ac.jp`

Abstract. Computational results are presented on micro-hologram diffraction for optical data storage using a finite element method. Retrieval of object light from a micro-hologram is formulated as an optical scattering problem in an infinite region. In order to overcome the difficulty of dealing with the infinite region a Dirichlet to Neumann (DtN) map is employed on an artificial boundary. By virtue of the DtN map reflection from the artificial boundary is effectively alleviated and non-reflecting boundary is obtained. Retrieval of the object light is computed for two different models.

Keywords. optical scattering, DtN map, finite element method, micro-hologram

1 Introduction

Holographic data storage using micro-holograms has been studied as a next generation optical data storage with terabyte capacity; see Eichler, et al. [3], and Kinoshita, et al. [5]. Retrieval of object light from a hologram is described as an optical scattering problem, which is stated by the Helmholtz equation in an infinite region.

In order to avoid computational difficulty in an infinite region, several techniques have been developed to transform the original problem into one in a bounded domain. They include Boundary Element Method (BEM) [8], hybrid finite element method with BEM coupling [7], Perfectly Matched Layer (PML) [1], Transparent Boundary Condition (TBC) [9], and Dirichlet to Neumann (DtN) map [4], [6]. To the best of our knowledge, DtN map has not been used for the wavelength of visible light, where the wave number is of order 10^7 In this paper, we apply a DtN map to our optical scattering problem and simulate retrieval of object light from a micro-hologram.

2 Formulation

Let Ω_B be a 2-dimensional transmissive scatterer with a smooth boundary Γ and an outward unit normal n; see Fig. 1. We assume the time harmonic field. Let u be the complex amplitude of a scalar component of the electric field of scattered light at visible wavelength. The scattering problem is

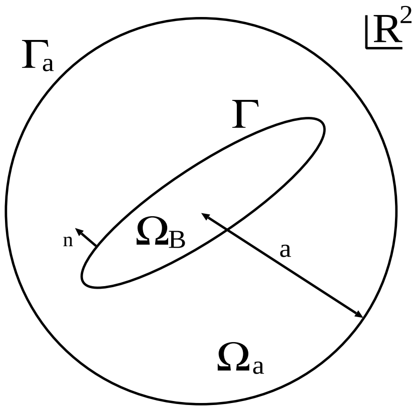

Fig.1 A scatterer Ω_B and an artificial boundary Γ_a.

formulated by the following Helmholtz equations in $\mathbb{R}^2$ according to [2], [9]; find $u : \mathbb{R}^2 \to \mathbb{C}$ such that

$$
\begin{cases}
-\Delta u - k_1^2 u = (\Delta + k_1^2) u^{\mathrm{inc}} & \text{in } \Omega_B, & \text{(1a)} \\
-\Delta u - k_0^2 u = 0 & \text{in } \Omega_B^c, & \text{(1b)} \\
[\,u\,] = 0 & \text{on } \Gamma, & \text{(1c)} \\
\left[\dfrac{\partial u}{\partial n} \right] = 0 & \text{on } \Gamma, & \text{(1d)} \\
\lim\limits_{r \to +\infty} \sqrt{r} \left(\dfrac{\partial u}{\partial r} - i k_0 u \right) = 0, & & \text{(1e)}
\end{cases}
$$

where k_0 (or k_1) is a wave number in the vacuum (or the medium), u^{inc} an incident light, $[\,.\,]$ a gap across Γ, and $r := |x|$ with the orthogonal coordinate system $x = (x_1, x_2)$ in $\mathbb{R}^2$.

Let Ω_a be a circle with the radius a (> 0), and let Γ_a be the boundary of Ω_a; see again Fig. 1. Suppose that the circle Ω_a includes Ω_B strictly. Let u^{inc} be an incident light. By introducing DtN map [4], the problem (1) become equivalent to the following one in Ω_a; find $u : \Omega_a \to \mathbb{C}$ such that

$$
\begin{cases}
-\Delta u - k_1^2 u = (\Delta + k_1^2) u^{\mathrm{inc}} & \text{in } \Omega_B, & \text{(2a)} \\
-\Delta u - k_0^2 u = 0 & \text{in } \Omega_a \backslash \Omega_B, & \text{(2b)} \\
[\,u\,] = 0 & \text{on } \Gamma, & \text{(2c)} \\
\left[\dfrac{\partial u}{\partial n} \right] = 0 & \text{on } \Gamma, & \text{(2d)} \\
\dfrac{\partial u}{\partial r} = -S u & \text{on } \Gamma_a. & \text{(2e)}
\end{cases}
$$

Here S is the Steklov–Poincaré operator defined by

$$
S u := -k_0 \sum_{n=-\infty}^{\infty} \frac{H_n^{(1)\prime}(k_0 a)}{H_n^{(1)}(k_0 a)}\, u_n(a)\, \phi_n(\theta),
$$

where (r, θ) is the polar coordinate system in $\mathbb{R}^2$, $H_n^{(1)}$ Hankel function of the first kind of order n, $\phi_n(\theta)$ the spherical harmonics defined by

$$
\phi_n(\theta) := \frac{1}{\sqrt{2\pi}}\, e^{in\theta}
$$

with the imaginary unit i, and u_n a Fourier coefficient defined by

$$u_n(a) := \int_0^{2\pi} u(a,\theta)\,\overline{\phi_n(\theta)}\; d\theta.$$

Let $L^2(\Omega_a)$ be the space of complex functions defined in Ω_a and square summable in Ω_a, and let $\|\,.\,\|_{0,\Omega_a}$ be its norm. For $m \in \mathbb{N}$, let $H^m(\Omega)$ be the space of complex functions in $L^2(\Omega_a)$ with derivatives up to the m th order, and let $\|\,.\,\|_{m,\Omega_a}$ be its norm. Set $V := H^1(\Omega_a)$. Moreover, bilinear forms a and s are defined by

$$a(u,v) := \int_{\Omega_a} (\nabla u\,\cdot \nabla \overline{v} - k^2 u\,\overline{v}\,)\; dx \qquad \forall u,v \in V,$$

$$s(u,v) := \int_{\Gamma_a} (Su)\,\overline{v}\; ds \qquad \forall u,v \in V,$$

and a linear functional f is defined by

$$\langle f, v\rangle := \int_{\Omega_a} f\,\overline{v}\; dx \qquad \forall v \in V.$$

Here, k is a piecewise constant function deinfed by

$$k(x) := \begin{cases} k_0 & \text{in } \Omega_a \backslash \Omega_B, \\ k_1 & \text{in } \Omega_B, \end{cases}$$

and f is a scattering potential defined by

$$f(x) := \begin{cases} 0 & \text{in } \Omega_a \backslash \Omega_B, \\ (\Delta + k_1^2)u^{\text{inc}} & \text{in } \Omega_B. \end{cases}$$

Note that simple calculations make the bilinear form s become

$$s(u,v) = -k_0\,a \sum_{n=-\infty}^{+\infty} \frac{H_n^{(1)\prime}(k_0 a)}{H_n^{(1)}(k_0 a)}\; u_n\,\overline{v_n}.$$

Now, the equation (2) can be written in a weak form as follows: find $u \in V$ such that

$$a(u,v) + s(u,v) = \langle f, v\rangle, \quad \forall v \in V. \tag{3}$$

3 Finite element approximation

Let $\{\mathscr{T}_h\}$ be a uniformly regular family of triangulation of $\overline{\Omega}_a$, where h stands for the maximum diameter of the triangles in $\mathscr{T}_h$. We set $\Omega_{ah} := \mathscr{T}_h$. By definition, let V_h be a finite dimensional subspace of V approximated by the conforming $P1$ elements. Moreover, the bilinear forms a and s, and the linear functional f are approximated by bilinear forms a_h and s_h^N, and a linear functional f_h defined by, for $u_h,\, v_h \in V_h$,

$$a_h(u_h, v_h) := \int_{\Omega_{ah}} (\nabla u_h\,\cdot \nabla \overline{v}_h - k^2 u_h\,\overline{v}_h)\; dx,$$

$$s_h^N(u_h, v_h) := -k_0\,a \sum_{n=-N}^{N} \frac{H_n^{(1)\prime}(k_0 a)}{H_n^{(1)}(k_0 a)}\; u_{hn}\,\overline{v}_{hn},$$

$$\langle f_h, v_h\rangle := \int_{\Omega_{ah}} (\Pi_h f)\,\overline{v}_h\; dx,$$

where N is a truncation number and $\Pi_h f$ denotes the $P1$ interpolant of f.

Then, a finite element problem corresponding to (3) is obtained as follows: find $u_h \in V_h$ such that

$$a_h(u_h, v_h) + s_h^N(u_h, v_h) = \langle f_h, v_h \rangle, \quad \forall v_h \in V_h. \tag{4}$$

Remark 1 Let D be a reflective scatterer with smooth boundary Γ. Then, the Helmholtz equation is solved in the exterior region $\mathbb{R}^2 \backslash D$. Suppose that a circle Ω_a includes D strictly. Then, we can obtain an equivalent formula as follows:

$$\begin{cases} -\Delta u - k_0^2 u = f & \text{in } \Omega_a \backslash D, & \text{(5a)} \\ u = g & \text{on } \Gamma, & \text{(5b)} \\ \dfrac{\partial u}{\partial r} = -Su & \text{on } \Gamma_a. & \text{(5c)} \end{cases}$$

Under apropriate assumptions, there exists a convergence result for a finite element scheme (4) corresponding to this problem; see [6].

4 Numerical examples

A micro-hologram is modulation of refractive indices of a holographic material created as a result of interference by two counter-propagating lights intersecting with each other. For a given micro-hologram, we compute scattered light with regard to an incident light. Let u_1 and u_2 be the reference light and the object light, respectively. The incident field is given by u^{inc}. Retrieving process is to obtain the object light upon irradiation of an incident light as a result of scattering from the micro-hologram.

In our numerical examples, we employed as the incident light u^{inc} plane wave $e^{ik_0 x}$, whereas u_1 and u_2 are represented by Gaussian beams. The scattering potential f becomes $(-k_0^2 + k_1^2)\, e^{ik_0 x}$ in Ω_B. The complex amplitude u is approximated by the conventional conforming $P1$ elements. Throughout this examples, the refractive indices are $n_0 = 1.5$ and $n_1 = 1.51$ and the wavelength in vacuum is $\lambda = 1$, i.e. the equations are nondimensionalized with respect to λ. The wave numbers then become

$$k_0 := \frac{2\pi n_0}{\lambda} \approx 9.425, \quad k_1 := \frac{2\pi n_1}{\lambda} \approx 9.488.$$

In order to solve the resultant linear systems, Conjugate Residual (CR) method was used. The computations were done by Core 2 Duo 3GHz CPU with 8GB memories.

4.1 Model A

The transmissive scatterer Ω_B is given by

$$\Omega_B = \{x \in \mathbb{R}^2;\ |u_1 + u_2|^2 \geq 0.5\},$$

which is a result of interference of two Gaussian beams that intersect at 90 degrees are considered:

$$u_1(x_1, x_2) = \frac{1}{2}\sqrt{\frac{x_R}{q(x_1)}}\,\exp\!\left(-\frac{ik_0 x_2^2}{2q(x_1)}\right)\exp(ik_0 x_1),$$
$$u_2(x_1, x_2) = \frac{1}{2}\sqrt{\frac{x_R}{q(x_2)}}\,\exp\!\left(-\frac{ik_0 x_1^2}{2q(x_2)}\right)\exp(-ik_0 x_2).$$

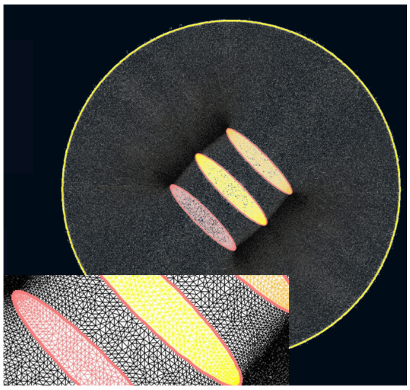

Fig.2 Model A and its triangulation.

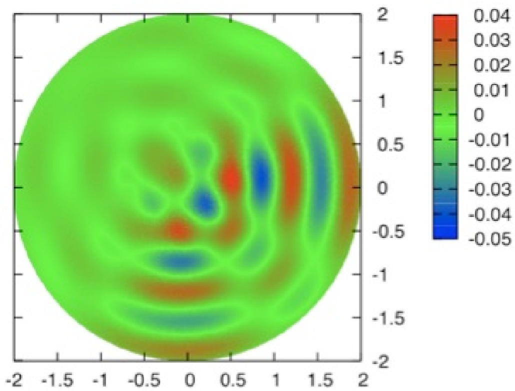

Fig.3 The real part of scattering waves in Model A.

The nondimensionalized complex beam parameter $q(x)$ is defined by $q(x) := x + ix_R$where x_R is the nondimensionalized Rayleigh range depending the waist size of the beam w_0,

$$w_0 = 1.22, \quad x_R := \frac{\pi w_0^2}{\lambda} \approx 4.676.$$

In this example the scatterer consists of three micro-ellipses orientated at 45 degrees as Fig. 2 depicts.

Fig. 2 also shows triangulation, in which the number of triangles is 105,578, and the number of nodal points is 53,046. The truncation number N of DtN map is 115. CPU time is about 1 hour.

Figs. 3–5 show the real part, the imaginary part, and absolute value of scattered light, respectively.

Retrieved light propagating along $-x_2$ axis, the direction of objective light, can be clearly seen as well as transmitted light along x_1 direction, reference light direction. No reflection from the artificial boundary was observed.

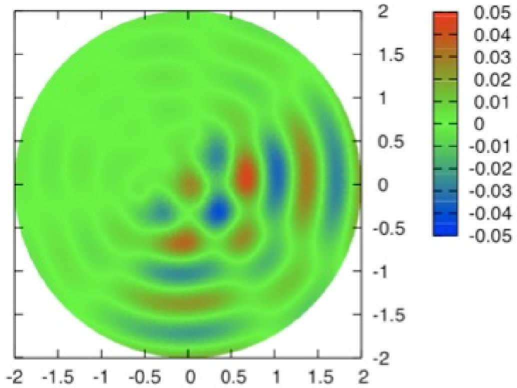

Fig.4 The imaginary part of scattering waves in Model A.

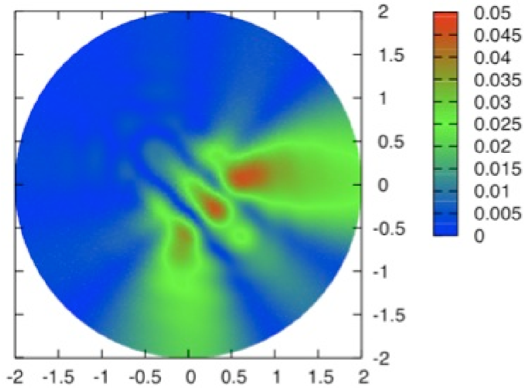

Fig.5 The absolute value of scattering waves in Model A.

4.2 Model B

In the next model, the scatterer Ω_B is represented by

$$\Omega_B = \{x \in \mathbb{R}^2;\ |u_1 + u_2|^2 \geq 0.5\},$$

which is created by two counter-propagating Gaussian beams:

$$u_1(x_1, x_2) = \frac{1}{2}\sqrt{\frac{x_R}{q(x_1)}}\exp\left(-\frac{ik_0 x_2^2}{2q(x_1)}\right)\exp(ik_0 x_1),$$
$$u_2(x_1, x_2) = \frac{1}{2}\sqrt{\frac{x_R}{q(x_1)}}\exp\left(-\frac{ik_0 x_2^2}{2q(x_1)}\right)\exp(-ik_0 x_1).$$

where $w_0 = 0.7176$ and $x_R := \pi w_0^2/\lambda \approx 1.618$.

As shown in Fig. 6 the scatterer Ω_B consists of seventeen micro-ellipses. The number of triangles is 585,019, and the number of nodal points is 1,169,012. The truncation number N of DtN map is 191. CPU time is about 3 hours.

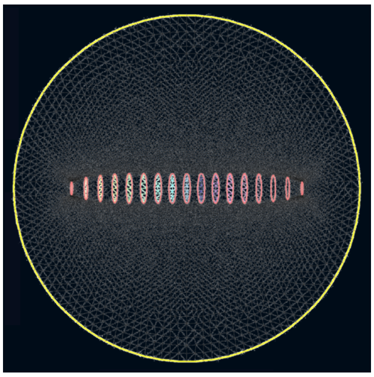

Fig.6　Model B and its triangulation.

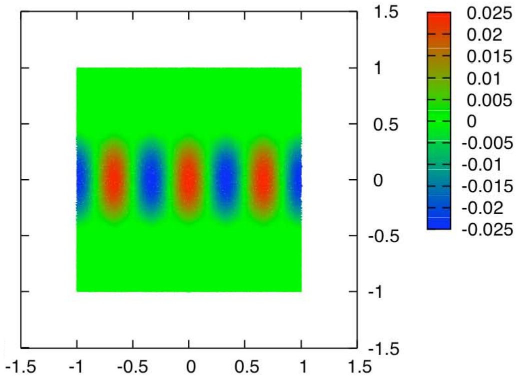

Fig.7　The real part of scattering waves in Model B.

Figs. 7–9 show the real part, the imaginary part, and the absolute value of the scattered field in the vicinity of the origin, respectively. Retrieval of the object light was successfully simulated. No reflection from the artificial boundary was observed.

5　Conclusion

A finite element method with a DtN map was successfully applied to an optical scattering problem. In computational results, no reflection from the artificial boundary was observed, which proved that the DtN map effectively reduced an infinte domain problem to a bounded domain problem even for the case of visible light.

Retrieval of the object light from a micro-hologram was qualitatively simulated as scattering of an incident reference light in two different configurations. It was confirmed that this method can be effectively used for analyses of holographic data storage based on the micro-hologram.

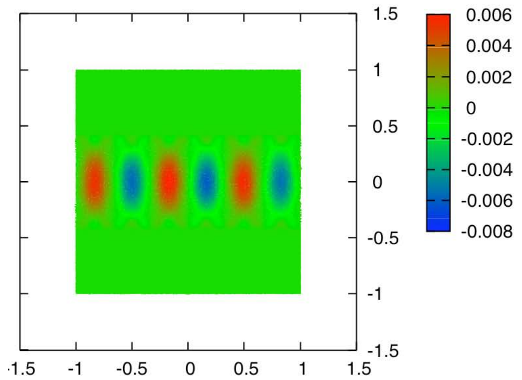

Fig.8 The imaginary part of scattering waves in Model B.

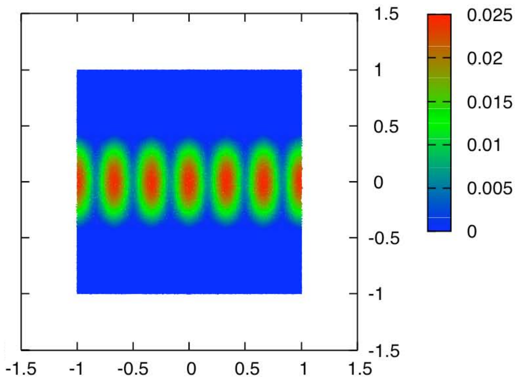

Fig.9 The absolute value of scattering waves in Model B.

Acknowledgments

The third author was supported by the Japan Society for the Promotion of Science under Grant-in-Aid for Scientific Research (S), No.20224001 and by the Ministry of Education, Culture, Sports, Science and Technology of Japan under Global COE Program, Mathematics for Industry. The fourth author was supported by the Japan Society for the Promotion of Science under Grant-in-Aid for Young Scientists (B), No.18740056. The authors would like to thank Panasonic Communications Co., Ltd. for the support to this study.

References

[1] J. P. Bérenger, A perfectly matched layer for the absorption of electromagnetic waves, J. Comput. Phys, **114** (1994), 185–200.

[2] M. Born and E. Wolf, Principles of optics, Cambridge University Press, 1999.

[3] H. J. Eichler et al., High-density disk storage by multiplexed microholograms, IEEE J. Sel. Top.

Quantum Electron, **4** (1998), 840–848.

[4] J. B. Keller, and D. Giovoli, Exact non-reflecting boundary conditions, J. Comput. Phys., **82** (1989), 172–192.

[5] N. Kinoshita, H. Shiino, N. Ishii, N. Shimidzu, and K. Kamijo, Integrated simulation technique for volume holographic memory using finite-difference time-domain method, Japanese J. Appl. Phys., **44** (2005), 3503–3507.

[6] D. Koyama, Error estimates of the DtN finite element method for the exterior Helmholtz problem, J. Comput. Appl. Math., **200** (2007), 21–31.

[7] M. S. Mirotznik, D. W. Prather, and J. N. Mait, A hybrid finite element-boundary element method for the analysis of diffractive elements, J. Modern Optics, **43** (1996), 1309–1321.

[8] D. W. Prather, Boundary integral methods applied to the analysis of diffractive optical elements, J. Opt. Soc. Am. A/ **14** (1997), 34–43.

[9] J. L. Volakis, A. Chatterjee, and L. C. Kempel, Finite element method for electromagnetics, IEEE Press, 1998

List of MI Preprint Series, Kyushu University

The Global COE Program
Math-for-Industry Education & Research Hub

MI

MI2008-1 Takahiro ITO, Shuichi INOKUCHI & Yoshihiro MIZOGUCHI
Abstract collision systems simulated by cellular automata

MI2008-2 Eiji ONODERA
The intial value problem for a third-order dispersive flow into compact almost Hermitian manifolds

MI2008-3 Hiroaki KIDO
On isosceles sets in the 4-dimensional Euclidean space

MI2008-4 Hirofumi NOTSU
Numerical computations of cavity flow problems by a pressure stabilized characteristic-curve finite element scheme

MI2008-5 Yoshiyasu OZEKI
Torsion points of abelian varieties with values in nfinite extensions over a p-adic field

MI2008-6 Yoshiyuki TOMIYAMA
Lifting Galois representations over arbitrary number fields

MI2008-7 Takehiro HIROTSU & Setsuo TANIGUCHI
The random walk model revisited

MI2008-8 Silvia GANDY, Masaaki KANNO, Hirokazu ANAI & Kazuhiro YOKOYAMA
Optimizing a particular real root of a polynomial by a special cylindrical algebraic decomposition

MI2008-9 Kazufumi KIMOTO, Sho MATSUMOTO & Masato WAKAYAMA
Alpha-determinant cyclic modules and Jacobi polynomials

MI2009-6 Kenji KAJIWARA & Yasuhiro OHTA
Bilinearization and Casorati determinant solutions to non-autonomous 1+1 dimensional discrete soliton equations

MI2009-7 Yoshiyuki KAGEI
Asymptotic behavior of solutions of the compressible Navier-Stokes equation around the plane Couette flow

MI2009-8 Shohei TATEISHI, Hidetoshi MATSUI & Sadanori KONISHI
Nonlinear regression modeling via the lasso-type regularization

MI2009-9 Takeshi TAKAISHI & Masato KIMURA
Phase field model for mode III crack growth in two dimensional elasticity

MI2009-10 Shingo SAITO
Generalisation of Mack's formula for claims reserving with arbitrary exponents for the variance assumption

MI2009-11 Kenji KAJIWARA, Masanobu KANEKO, Atsushi NOBE & Teruhisa TSUDA
Ultradiscretization of a solvable two-dimensional chaotic map associated with the Hesse cubic curve

MI2009-12 Tetsu MASUDA
Hypergeometric τ-functions of the q-Painlevé system of type $E_8^{(1)}$

MI2009-13 Hidenao IWANE, Hitoshi YANAMI, Hirokazu ANAI & Kazuhiro YOKOYAMA
A Practical Implementation of a Symbolic-Numeric Cylindrical Algebraic Decomposition for Quantifier Elimination

MI2009-14 Yasunori MAEKAWA
On Gaussian decay estimates of solutions to some linear elliptic equations and its applications

MI2009-15 Yuya ISHIHARA & Yoshiyuki KAGEI
Large time behavior of the semigroup on L^p spaces associated with the linearized compressible Navier-Stokes equation in a cylindrical domain

MI2009-16 Chikashi ARITA, Atsuo KUNIBA, Kazumitsu SAKAI & Tsuyoshi SAWABE
Spectrum in multi-species asymmetric simple exclusion process on a ring

MI2009-17 Masato WAKAYAMA & Keitaro YAMAMOTO
Non-linear algebraic differential equations satisfied by certain family of elliptic functions

MI2009-18 Me Me NAING & Yasuhide FUKUMOTO
Local Instability of an Elliptical Flow Subjected to a Coriolis Force

MI2009-19 Mitsunori KAYANO & Sadanori KONISHI
Sparse functional principal component analysis via regularized basis expansions and its application

MI2009-20 Shuichi KAWANO & Sadanori KONISHI
Semi-supervised logistic discrimination via regularized Gaussian basis expansions

MI2009-21 Hiroshi YOSHIDA, Yoshihiro MIWA & Masanobu KANEKO
Elliptic curves and Fibonacci numbers arising from Lindenmayer system with symbolic computations

MI2009-22 Eiji ONODERA
A remark on the global existence of a third order dispersive flow into locally Hermitian symmetric spaces

MI2009-23 Stjepan LUGOMER & Yasuhide FUKUMOTO
Generation of ribbons, helicoids and complex scherk surface in laser-matter Interactions

MI2009-24 Yu KAWAKAMI
Recent progress in value distribution of the hyperbolic Gauss map

MI2009-25 Takehiko KINOSHITA & Mitsuhiro T. NAKAO
On very accurate enclosure of the optimal constant in the a priori error estimates for H_0^2-projection

MI2009-26 Manabu YOSHIDA
Ramification of local fields and Fontaine's property (Pm)

MI2009-27 Yu KAWAKAMI
Value distribution of the hyperbolic Gauss maps for flat fronts in hyperbolic three-space

MI2009-28 Masahisa TABATA
Numerical simulation of fluid movement in an hourglass by an energy-stable finite element scheme

MI2009-29 Yoshiyuki KAGEI & Yasunori MAEKAWA
Asymptotic behaviors of solutions to evolution equations in the presence of translation and scaling invariance

MI2009-30 Yoshiyuki KAGEI & Yasunori MAEKAWA
On asymptotic behaviors of solutions to parabolic systems modelling chemotaxis

MI2009-31 Masato WAKAYAMA & Yoshinori YAMASAKI
Hecke's zeros and higher depth determinants

MI2009-32 Olivier PIRONNEAU & Masahisa TABATA
Stability and convergence of a Galerkin-characteristics finite element scheme of lumped mass type

MI2009-33 Chikashi ARITA
Queueing process with excluded-volume effect

MI2009-34 Kenji KAJIWARA, Nobutaka NAKAZONO and Teruhisa TSUDA
Projective reduction of the discrete Painlev'e system of type$(A_2 + A_1)^{(1)}$

MI2009-35 Yosuke MIZUYAMA, Takamasa SHINDE, Masahisa TABATA and Daisuke TAGAMI
Finite element computation for scattering problems of micro-hologram using DtN map